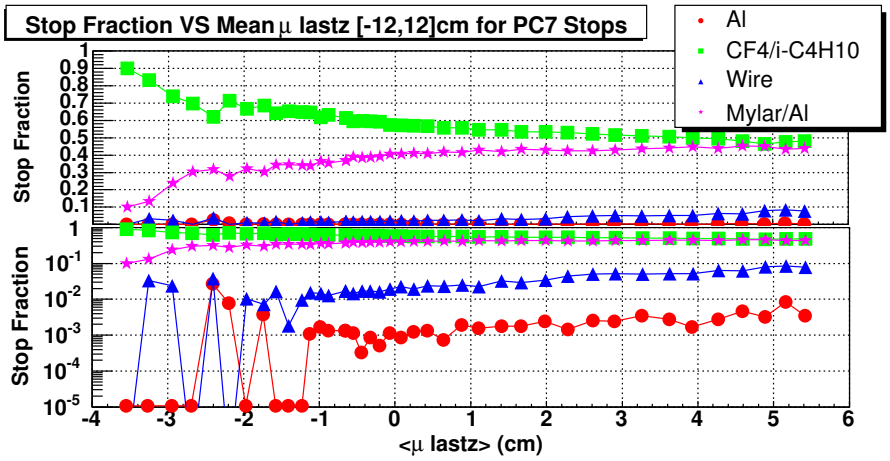

Figure 6.4: Plot of the fraction of muons stopping in Aluminum (Al), Gold plated Tungsten wire, CF4/i-C4H10, and Aluminized Mylar foil for muons with last TDC hit in PC7, versus the mean muon stopping z coordinate between -12.cm and 12.cm from TDC information.

Depolarization in Aluminum

A depolarization versus decay time has been observed for muons stopping in our aluminum target. Plots of the polarization estimate from an asymmetry analysis of the 2004 data at the top, and 2004 MC at the bottom are shown in Figure 6.5. The depolarization rate cannot be explained solely by muons that stop in gas rather than aluminum. Models for depolarization in metal are either of an exponential or gaussian form. Calculations have shown that the only practical form is an exponential, since the effects of the other models cannot be very large.

The difference between the two model extrapolations is $2.4 \times 10^{-}3$, and this difference is the *correction* that we need to apply to our MC to data fits, since the MC was generated with a gaussian form, and we want to fit to an exponential form. An estimate of the extrapolation error is obtained by comparing fits with the slope as a fit parameter, and fits with the slope fixed as shown in Figure 6.6. The error due to extrapolation is: $\sqrt{0.00099^2 - 0.00049^2} = 0.00085$.

6.1.2 Fringe Field Depolarization

In this section the sensitivity and systematic error of $P_\mu \xi$ due to uncertainty in beam position and angle is estimated. The uncertainty in beam measurement is estimated in the apparatus section describing the TEC. The uncertainty in the beam position was estimated to be $\pm 2mm$, and the uncertainty in the beam angle was estimated to be $\pm 5mrad$. While this seems like a fairly large

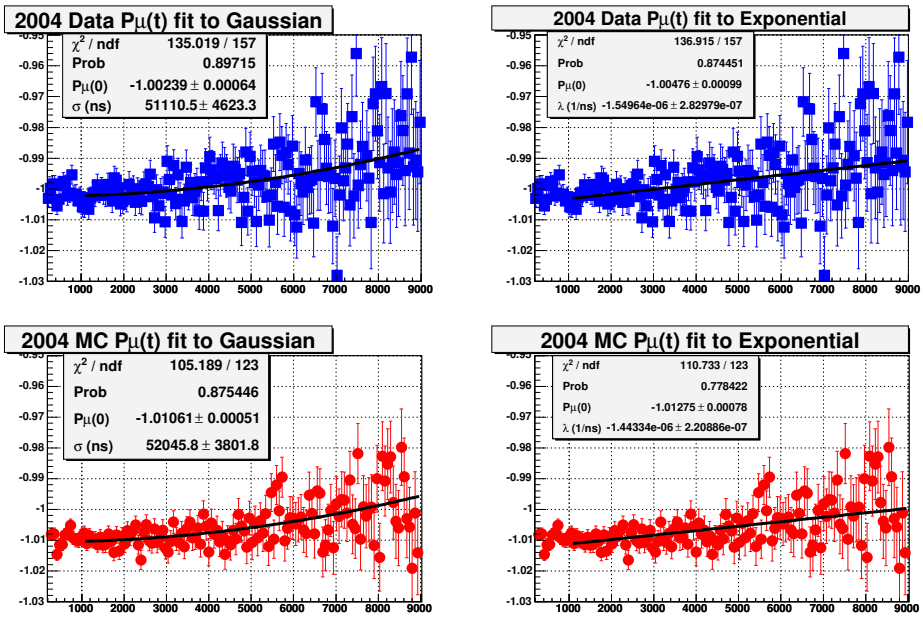

Figure 6.5: Plot of the polarization estimate from an asymmetry analysis of the 2004 data at the top, and 2004 MC at the bottom. The distributions are fit to a gaussian on the left and to an exponential on the right.

uncertainty it is in line with discrepancies between the muon beam position in the detector in MC and data as shown in Figure 6.7.

To estimate the sensitivity to fringe field depolarization, the beam input into MC was scanned over the range $\pm 2cm$ and $\pm 20mrad$ in both x and y. The result of this scan shows that the polarization versus beam shift can be approximated by a quadratic polynomial. The scan results are shown in Figure 6.8.

The quadratic that was fit to is given in Equation 6.9, where the x, y, dx and dy represent the shifts in the positions and angles.

$$P_\mu(x, y, dx, dy) = P_{max} - A((dx - x_0)^2 + (dy - y_0)^2) \tag{6.9}$$

The fit constants P_{max} and A were roughly independent of the shift in x and y, while the fit constants x_0 and y_0 were found to be functions of x and y. The polynomial fits are shown in Figure 6.9.

Fits to x_0 versus x and y, and y_0 versus x and y can be done to find the constants in the linear equations:

$$x_0 = x_{00} + x_{0x}x \tag{6.10}$$
$$x_0 = x_{00} + x_{0y}y \tag{6.11}$$
$$y_0 = y_{00} + y_{0x}x \tag{6.12}$$
$$y_0 = y_{00} + y_{0y}y \tag{6.13}$$

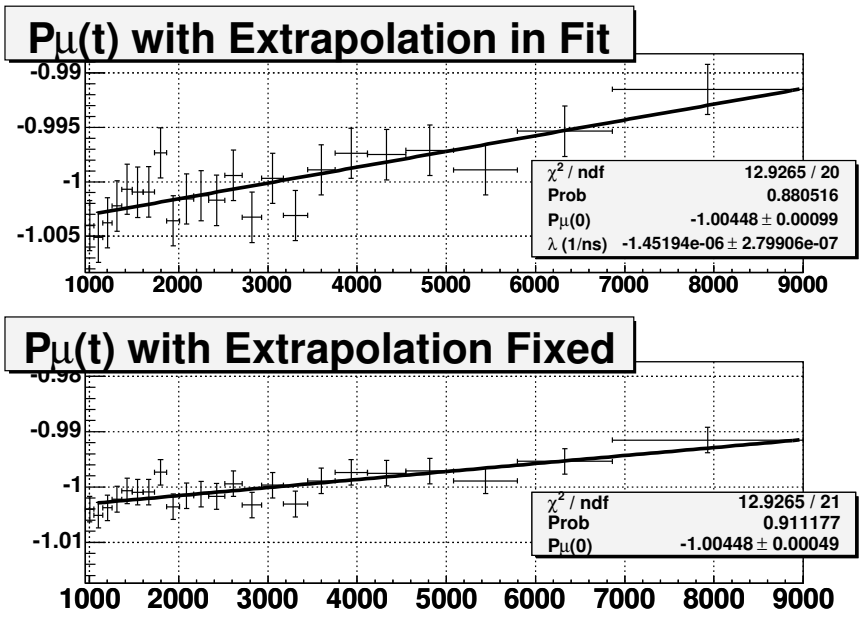

Figure 6.6: Plot of the polarization estimate from an asymmetry analysis of the 2004 data fit to an exponential with the slope as a fit parameter in the top figure, and with the slope fixed in the bottom figure.

The fits to these linear equations are shown in Figure 6.10.

The overall four dimensional polynomial can be written out:

$$P_\mu(x,y,dx,dy) = P_{max} - A((dx - x_{00} - x_{0x}x - x_{0y}y)^2 + (dy - y_{00} = y_{0x}x - y_{0y}y0)^2) \tag{6.14}$$

The constants in this polynomial for the standard beam tune are summarized in Table 6.2.

The four dimensional polynomial can be used to plot the sensitivity of the polarization to the estimated shifts in the beam. The result is that for an uncertainty in the beam position of $\pm 2mm$, and uncertainty in the beam angle of $\pm 5mrad$, the systematic error in $P_\mu \xi$ ± 0.0015. The plot of the four dimensional polynomial used for this error estimate is shown in Figure 6.12.

6.1.3 Depolarization in the Muon Production Target

$\Delta(p)/p$ of 1% (FWHM) means that we have a range of roughly 29.4 to 29.8MeV/c at our 29.6MeV/c setting, if you are conservative to include a little extra for tails of the non-gaussian distribution. This is a range of 0.4MeV/c.

$\Delta(p)/\Delta(x)$ for this momentum is about 39.5$MeV/c/(g/cm^2)$ for Cu (similar to stainless steel) or 55$MeV/c/(g/cm^2)$ for carbon. Thus the difference in

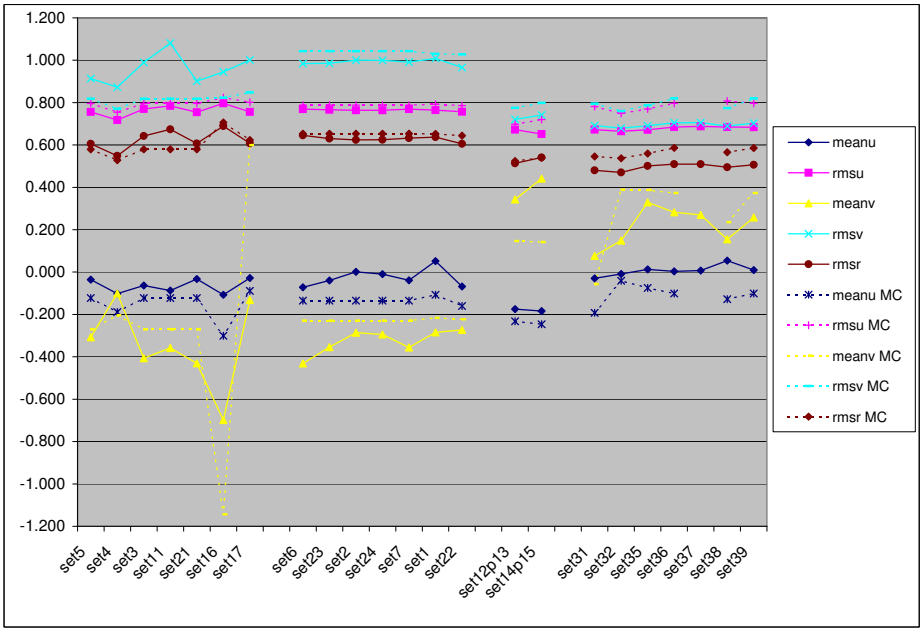

Figure 6.7: This plot shows the match between the mean beam positions and RMS at the stopping target. The match between the two is shown for each of the data sets being considered. Units on vertical scale are centimeters.

thickness corresponding to $0.4MeV/c$, which is a good estimate of the effective maximum depth from which our muons are born, is $0.010g/cm^2$ (ss) or $0.007g/cm^2$ (graphite). Using densities of 8 and $2.26g/cm^3$ respectively, the depths are $0.0012cm$ (ss) and 0.003 cm (graphite). Note that this is $30\mu m$ for the Graphite target.

Using the PDG multiple scattering formula, the multiple scattering angle in Graphite can be estimated. X_0 is $42.7g/cm^2$, so $x/X_0 = 0.007/42.7 = 0.00016$, which is well below the quoted range of validity for the multiple scattering formula. Working it out anyways for $\beta = 0.265$ gives 0.0052 radians for $theta_0$.

An estimate of the depolarization in the small angle approximation, and averaging over phi angles which give a reduction of two times is estimated by $(theta_0)^2/4$. This works out to a contribution $< 10^{-5}$.

6.1.4 Background Muon Contamination

A contribution to the depolarization is contamination from unpolarized background muons. Strong evidence for this is found in 2002 data where the muons were stopped further upstream than nominal. In this set a reduced polarization is observed for muons whose last hit was in PC7 or PC8.

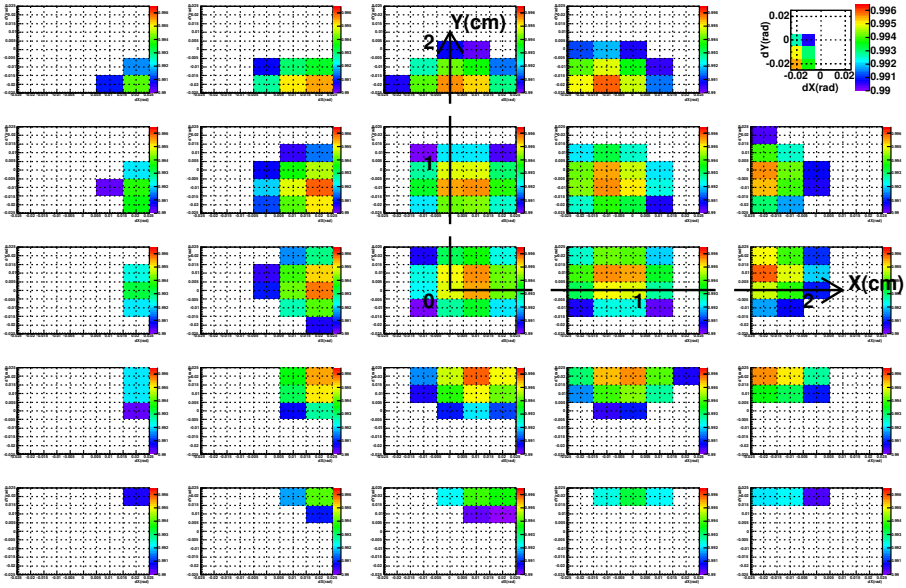

Figure 6.8: Fringe Field Sensitivity MC Scan showing the mean spin along the z axis for muons that stop in the target, where red is the highest polarization of 0.965, and blue is the lowest polarization of 0.99. An unshaded or white square is lower polarization than 0.99. Each of the 25 plots shown here is a polarization for each shift in dY versus dX from +20 mrad to -20mrad. The middle plot is for an unshifted beam, plots on the first row are for the beam shifted up by 2cm at the TEC, the second row shifted up by 1cm, and so on filling the matrix of beam shifts in X and Y from +2cm to -2cm.

It is expected that nearly all of the surface muons will stop in or before the target, meaning that the stops observed in PC7 and PC8 are likely due to these background muons. An estimate for the contamination is done in the following way. The data was modeled in GEANT as a combination of a standard geant run with polarized surface muons, and a special run with muons arising from 29.6MeV/c pion decays in channel. Figure 6.13 shows the comparison of MC and data distributions of muon last plane hit before and after adding pions to the beam.

Using these simulations, the fraction of muon stops due to the pions relative to surface muons is summarized for the 2002, 2003, and 2004 data in Table 6.3. The maximum polarization change is calculated for the case where the background muons have polarization opposite to surface muons. These estimates say that the systematic uncertainty in $P_\mu \xi$ due to background muons in 2003 and 2004 data is better than ± 0.00018.

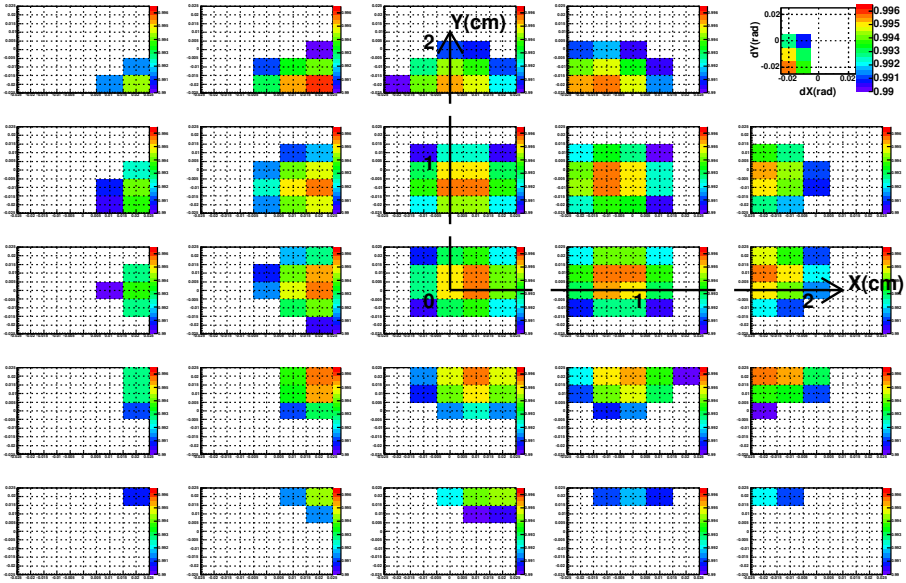

Figure 6.9: Plots showing the two dimensional quadratic fits of the polarization versus x, y, dx, and dy. The colouring and order of the plots is the same as described in Figure 6.8.

6.1.5 Proton Beam Stability

The movement of the muon beam when the proton beam on the production target was moved. The result is that $d\bar{y}_\mu/dy_p \approx 0.25$, and $d\bar{x}_\mu/dx_p \approx 0.5$. Movement of the proton beam by $\pm 1mm$ resulted in a change in the muon beam $\overline{dX}$ of $0.2mrad$, and the change in $\overline{dY}$ was less than $1.3mrad$

Monitoring of the beam position is done using roughly weekly low intensity target scans, where about $1\mu A$ of proton beam is steered both vertically and horizontally. Vertical steering of the protons is done with steering magnet labelled 1ASM4 (SM4), and horizontal steering with 1ASM5 (SM5). The calibration of the movement of the beam is with "protect monitor" plates located 2.5 mm to either side of the nominal proton beam steered centered. The setting of these steering magnets is monitored in our slow controls. The variation in position of the proton beam over the production data taking estimated from these history plots is 0.25mm vertically and 0.1mm horizontally.

From these numbers, the maximum movement of the muon beam due to proton beam movements is 0.063mm vertically and 0.025mm horizontally. The change in angle of the muon beam due to proton beam movement is within $0.08mrad$ vertically and $0.01mrad$ horizontally. The systematic error due to these beam movements is estimated using a plot similar to Figure 6.12. The result is that the systematic error due to proton beam stability is $\pm 0.02 \times 10^{-3}$.

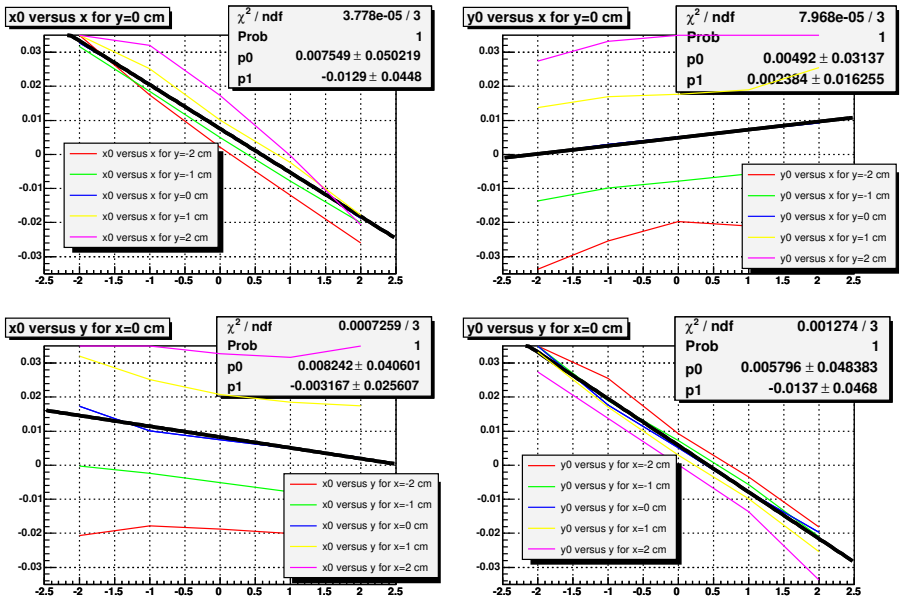

Figure 6.10: Fits of x0 versus x, x0 versus y, y0 versus x and y0 versus y used to obtain constants in the four dimensional polarization polynomial.

Parameter	Nominal	Aperture	Units
P_{max}	0.9958	0.9976	
A	-9.796	-10.536	$rad^{-}2$
x_{00}	0.0075	0.0067	rad
x_{0x}	-0.0129	-0.0121	rad/cm
x_{0y}	-0.0032	-0.0021	rad/cm
y_{00}	0.0058	0.0038	rad
y_{0x}	0.0024	0.0002	rad/cm
y_{0y}	-0.0137	-0.0122	rad/cm

Table 6.2: Beam polarization polynomial parameters from fit to MC scans of the different beam tunes.

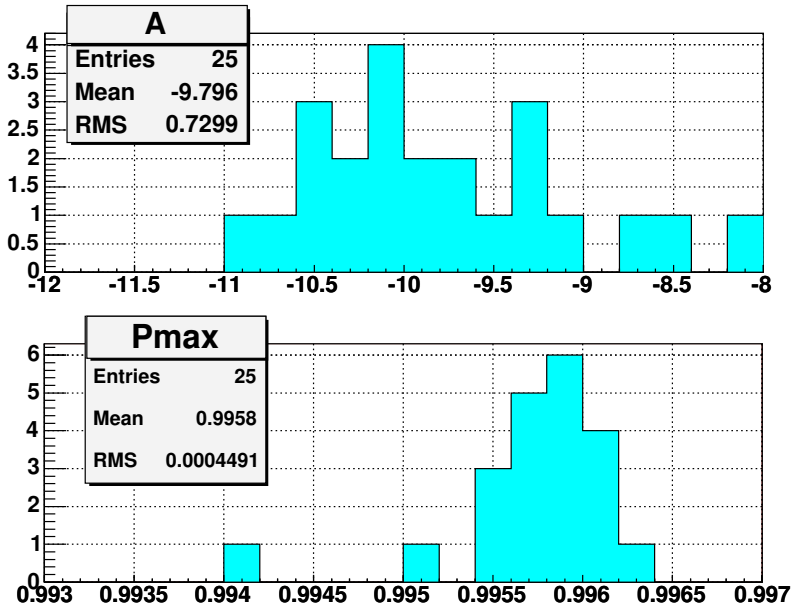

Figure 6.11: Histogram of the fit parameters A and pmax from fits to each of the 25 plots of polarization versus shift in dX and dY angle.

Data Type	f_{PC5}	f_{target}	f_{PC7}	$\max \Delta P_\mu$
2002 Nominal (Set 2)	0.009106	0.000364	0.000669	0.00072
2002 Upstream (Set 4)	0.009027	0.002793	0.012078	0.00240
2003 Nominal (Set 14)	0.000134	0.000013	0.000040	0.00003
2004 Nominal (Set 35)	0.001110	0.000088	0.000798	0.00018

Table 6.3: Fractions of background muons relative to surface muons for muons stopping in PC5, the target, and PC7. For the target stops the maximum effect on polarization is estimated.

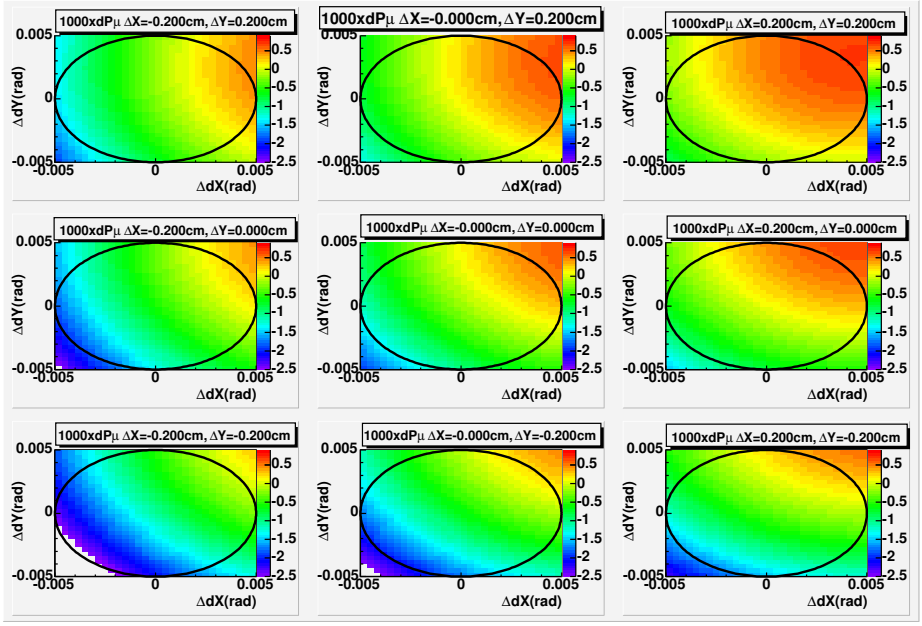

Figure 6.12: Plot used to estimate the fringe field systematic error due to uncertainty in the beam position of $\pm 2mm$, and uncertainty in the beam angle of $\pm 5mrad$.

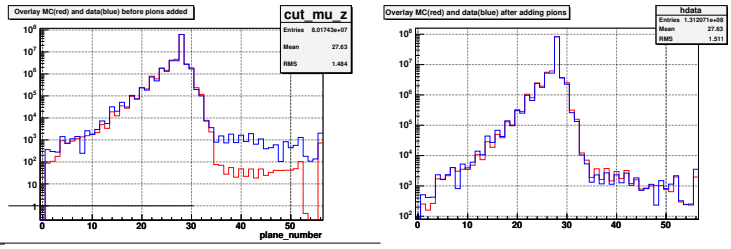

Figure 6.13: Overlay of the data set 35 and MC gen235 last plane hit histogram before adding muon stops from pions in the beam on the left. The same histograms but with pions added at the level of to the beam is shown on the right.

6.2 Systematic Error Due to Chamber Response

- DC efficiency (± 0.02)
- PC efficiency (± 0.01)
- Dead zone (± 0.26)
- Long drift times (± 0.17)
- HV variations (± 0.03)
- Temperature and pressure (0.24 ± 0.14)
- Foil bulges (0.89 ± 0.56)
- Crosstalk (± 0.04)
- t0 variations (0.49 ± 0.09)

6.3 Systematic Error Due to Spectrometer Alignment

- Translations (± 0.02)
- Rotations (0.1 ± 0.01)
- z (± 0.09)
- B field to detector axis (± 0.46)